pH controlled sensitive and selective detection of Cr(III) and Mn(II) by clove (*S. Aromaticum*) reduced and stabilized silver nanospheres†

Priyanka Joshi[a], Manjula Nair[b] and Dinesh Kumar[a*]

[a]Department of Chemistry, Banasthali University, Rajasthan-304022, India

[b]American College of Dubai–36778, UAE

Graphical abstract

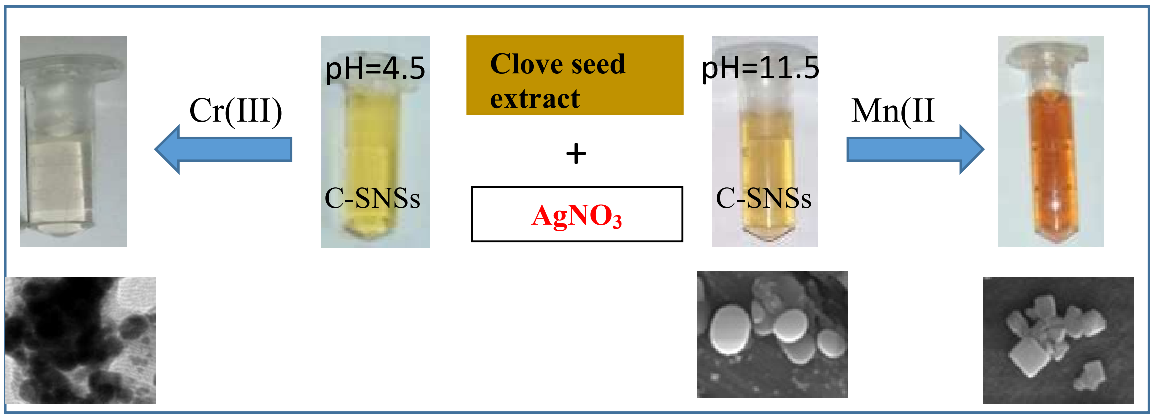

Abstract

The colorimetric detection of toxic metal ions based on silver nanoparticles (AgNPs) has received significant attention due to their distance dependent optical properties. Our study reports a new, green, selective and sensitive colorimetric detection method for Cr(III) and Mn(II) by clove silver nanospheres (C-SNSs) synthesized at two different pH values 4.5 and 11.5. At pH 4.5, C-SNSs gradually aggregated in the presence of Cr(III) ions and showed a

*Corresponding author: E-mail: dsbchoudhary2002@gmail.com

†Electronic supplementary information (ESI) available: Size distribution of C-SNSs at pH 4.5 in the absence and presence of Cr(III) ions and size distribution of C-SNSs at pH 11.5 in the absence and presence of Mn(II) ions. Zeta potential distribution of C-SNSs at pH 4.5 and 11.5 and zeta potential distribution of C-SNSs at pH 4.5 before (a) and after (b) interaction with Cr(III) ions and zeta potential distribution of C-SNSs at pH 11.5 before (c) and after (d) interaction with Mn(II) ions.

color change from light yellow to colorless. At pH 11.5, they showed rapid aggregation, not only with a colorimetric change from dark yellow to reddish brown, but also with an alteration in morphology of spheres to square pyramidal in the presence of Mn(II) ions. Cr(III) and Mn(II) ions were detected using colorimetry and spectrometry. Under optimized conditions, our method showed better selectivity for Cr(III) and Mn(II) ions as compared to other metal ions. The lowest limit of detections (LODs) of C-SNSs was 0.20 μM for both Cr(III) and Mn(II), which is significantly lower than the Environmental Protection Agency (EPA) permissible limits of 1.92 μM for Cr(III) and 0.91 μM for Mn(II).

Introduction

People today are more informed about environmental pollution and health hazards. Environment contamination by heavy metal ions Hg(II), Cd(II), Pb(II), As(III), Mn(II), Cr(III), Cr(VI) etc has been a major concern worldwide since decades. Heavy metal ions have received much attention as they are hazardous, both to human beings and the environment[1-4]. Though some heavy metal ions are essential for normal physiological functions of the human body, at elevated levels they have an adverse effect on human health and environment. For example, chromium is one of the trace elements *in–vivo* and usually presents as trivalent Cr(III) and hexavalent Cr(VI) ions in the environment. Cr(III) has a great impact on the metabolism of carbohydrates, fats, proteins, nucleic acids, and the formation of hemoglobin of red cells[5]. However, at elevated levels Cr(III) (>50-200 mg dl) can bind to DNA thereby affecting the cellular structures and damaging the cellular components that may even lead to mutation and cancer[6],[7]. Both the chromium species enter the environment as a result of effluent discharge from tanning industries, electroplating, cooling water towers, oxidative dyeing, chemical industries and steel works[8]. Manganese is essential for humans as its deficiency affects metabolism of fats and lipids. Lack of adequate Mn also causes skeletal abnormalities, bone demineralization, ataxia syndrome, and Perth's disease[9,10]. Over exposure to manganese can cause manganism and learning disabilities in children[11,12]. Hence, there is an urgent need for a highly sensitive and selective method for the detection of Cr(III)and Mn(II) ions in both environmental and biological samples[13,14]. These heavy metal ions have been detected previously by various methods like electro analytical sensing[15,16], electrospray ionization mass spectroscopy (EIMS)[17,18], high performance liquid chromatography (HPLC)[19-21], inductively coupled plasma mass spectroscopy (ICPMS)[22-24] and atomic absorption spectrometry (AAS)[25-27]. These are reliable techniques for detection; however, they have limitations with regard to simplicity, selectivity, portability and analysis time[11,28]. To overcome these problems, nanomaterial based sensors have been developed for detection of Cr(III) and Mn(II). In this order, unaltered SNSs have been used as the fluorescence probe for the detection of nanomolar chromium[29]. Glutathione stabilized fluorescent gold nanoclusters have been employed for sensing of Cr(III) and Cr(VI)[30]. Fluorescence quenching immune chromatographic nanosensor has been used for the detection of the chromium ion[31]. Surface changed or unchanged plasmonic nanoparticles have emerged as useful nanosensors for the selective sensing of Cr(III)and Mn(II)[32-37]. Although these methods are highly selective and sensitive, but they are energy and capital intensive, employ toxic chemicals, nonpolar solvents and synthetic additives or capping agents, which limits their applications[38]. Detection of metal toxicants in effluents is the main objective of the sensor. But, if the sensors themselves are toxic in nature, it does not serve the purpose. This has made researchers turn toward "green" chemistry and bioprocesses[39,40]. The key impact of "green nanoscience" includes ease of availability, non-pathogenicity, reduction in synthetic steps, easy recovery, low energy requirement, thus making them a preferred choice over the chemical methods[41]. Previously, Ha et al synthesized *Xanthoceras Sorbifola Tannin* attached gold nanoparticles (AuNPs) for the sensing of Cr(III) ion with a detection limit of 3 μM[42]. In continuation of researchers' interest in the development of green nanoparticles[43], we have synthesized C–SNSs at ambient conditions in aqueous media. The synthesized SNSs are highly selective for Cr(III) and Mn(II) ions over other alkali metals, alkaline earth and transition metals with a detection limit of 0.20 μM for both Cr(III) and Mn(II) which is significantly lower than the EPA permissible limits[44,45]. Thus, these findings provide a promising green analytical method for the detection of Cr(III) and Mn(II) toxic metal ions simultaneously from aqueous systems.

Experimental

Chemical and Materials

All the solutions were prepared with Milli–Q water. Silver nitrate ($AgNO_3$, 99.8%) was purchased from Sigma Aldrich. All metal salts, like $CaCl_2$, $CdCl_2$, $CuSO_4$, $HgCl_2$, $ZnCl_2$, $NiCl_2$, $Pb(CH_3COO)_2$, KCl, $CoCl_2$, $FeCl_3$, $K_2Cr_2O_7$, $BaCl_2$, $MnCl_2$, $AlCl_3$, $CrCl_3$, and NaOH were procured from Sigma Aldrich and Merck Pvt. Ltd, India. The solutions were prepared by mixing the required amounts of salts in 100 mL Mill–Q water and further diluted as per requirement. Glassware was thoroughly cleaned with aqua regia and rinsed with Mill–Q water prior to use. All chemicals were used as received.

Preparation of C-SNSs

Clove *(Syzigium aromaticum)* seeds were purchased from the local market. Seeds were ground into powder and stirred in a 250 mL beaker with 100 mL of Milli–Q water at 35 ℃ for 2 h. After agitation, the color of the solution changed to dark brown. The extract was filtered using Whatman No. 1 filter paper (pore size 25 μM), and stored in refrigerator prior to its use for the synthesis of SNSs.

We synthesized C-SNSs at pH 4.5 and 11.5 with slight modifications in previous report[46] by reducing $AgNO_3$ with clove seed extract at room temperature. To synthesize detection probe at pH 4.5, 50 mL solution of $AgNO_3$ (1 mM) was mixed with various volumes (50 to 850 μL) of clove seed extract followed by stirring for a few hours. The solution turned from colorless to light yellow. Similarly, detection probe was also synthesized at pH 11.5 by adjusting pH using NaOH. Solution turned from colorless to dark yellow. The detection probe solutions were stored under ambient conditions until used.

Colorimetric Detection of Cr(III) and Mn(II) Ions

The colorimetric detection of Cr(III) and Mn(II) was carried out by detection probe synthesized at pH 4.5 and 11.5, respectively. 200 μL aqueous solution of both Cr(III) and Mn(II) of different concentrations were separately added into 800 μL of respective detection probe solutions. The detection systems were kept at room temperature for 30 min and then characterized by dual strategies namely colorimetry and spectrometry.

Instrument

Optical absorption spectra were recorded using a lab India 3000$^+$ UV–vis spectrophotometer with 1 cm quartz cell by using Mill–Q water as blank for the background correction. Surface morphology was determined by scanning electron microscopy (SEM), and transmission electron microscopy (TEM). Zeta potential and average particle diameter were determined on a nanoseries–ZS90, Malvern instrument.

Result and Discussion

Stability of C-SNSs

In colorimetry, the stability of detection system under different conditions is of great importance. Therefore, stability of the C-SNSs was evaluated by UV-vis spectroscopy in terms of pH, volume of clove seed extract and time. First, the stability of C-SNSs was studied at pH range of 4.5-13 (Figure 1a). The pH adjustment showed a slight change in color of C-SNSs solution upto pH 11.5. Thereafter, no change in colour was observed upon increasing the pH to 13. The color distinction was reflected by surface plasmon resonance (SPR) spectra. The intensity and sharpness of SPR band continuously increased with a blue shift from 424-407 nm on increasing pH from 4.5 to 11.5. This trend confirms that a stable dispersion of C-SNSs was formed at pH 11.5. As the initial pH of synthesized SNSs was 4.5 and they were maximally stable at pH 11.5, we used C-SNSs at pH 4.5 and 11.5 to check their suitability for the colorimetric detection.

Further, to know the effect of volume of clove seed extract on the stability of C–SNSs, different volumes of clove seed extract (50-850μL) were added to $AgNO_3$ solution. Upon varying the volume, the color of $AgNO_3$ solution changed from colorless to yellow. These results were further confirmed by SPR spectra. As shown in Figure 1b, the intensity of SPR peak was increased on increasing the volume of clove seed extract from 50-450 μL. When the volume was increased from 650–850 μL an immediate change in color from yellow to reddish brown was observed with broadening of peak. Therefore, we selected 450 μL of clove seed extract as the best optimal volume to stabilized C-SNSs.

Finally, an important factor which needed to be controlled during the synthesis of C-SNSs was the reaction time. As the reaction time was increased from 5-120 min, transparent solution of $AgNO_3$ started to darken. It is apparent from Figure 1c, that after 5 min, no optical absorption was shown in the range 400–500 nm, only a shoulder was observed at 385 nm. With time, shoulder disappeared and a new peak started to appear at 424 nm, which became sharp at 65 min. The intensity of peak increased with reaction time from 65−120 min without any significant change in the position. It indicates the reduction of Ag^+ ion into Ag atoms was completed within 65 min.

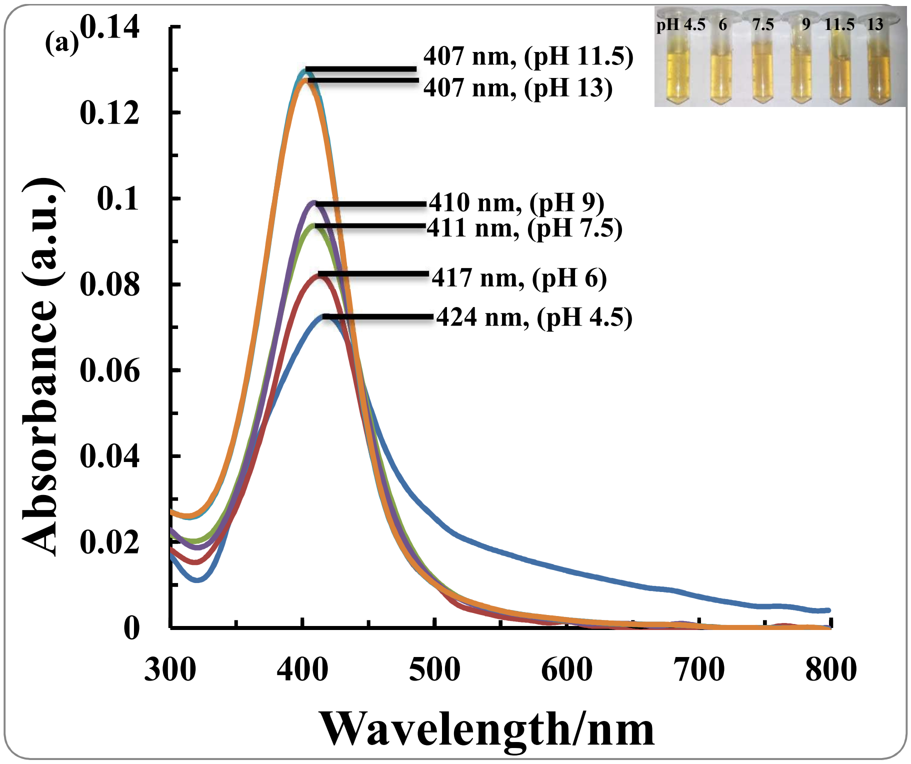
(a)
pH 4.5
6
7.5
9
11.5
13
407 nm, (pH 11.5)
407 nm, (pH 13)
410 nm, (pH 9)
411 nm, (pH 7.5)
417 nm, (pH 6)
424 nm, (pH 4.5)
Absorbance (a.u.)
0.14
0.12
0.1
0.08
0.06
0.04
0.02
0
300
400
500
600
700
800
Wavelength/nm

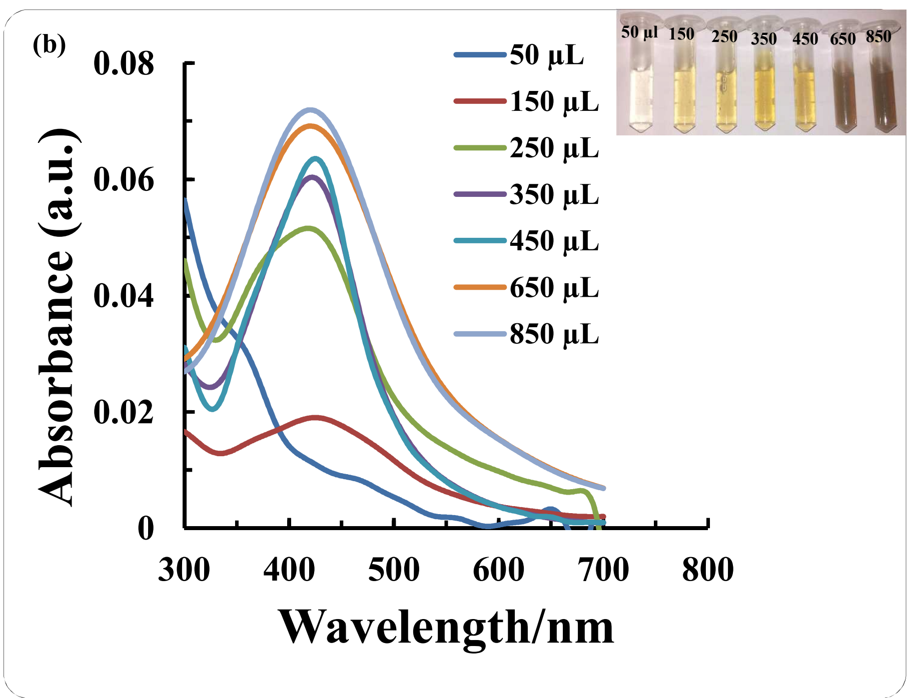
(b)
50 µl
150
250
350
450
650
850
50 µL
150 µL
250 µL
350 µL
450 µL
650 µL
850 µL
Absorbance (a.u.)
0.08
0.06
0.04
0.02
0
300
400
500
600
700
800
Wavelength/nm

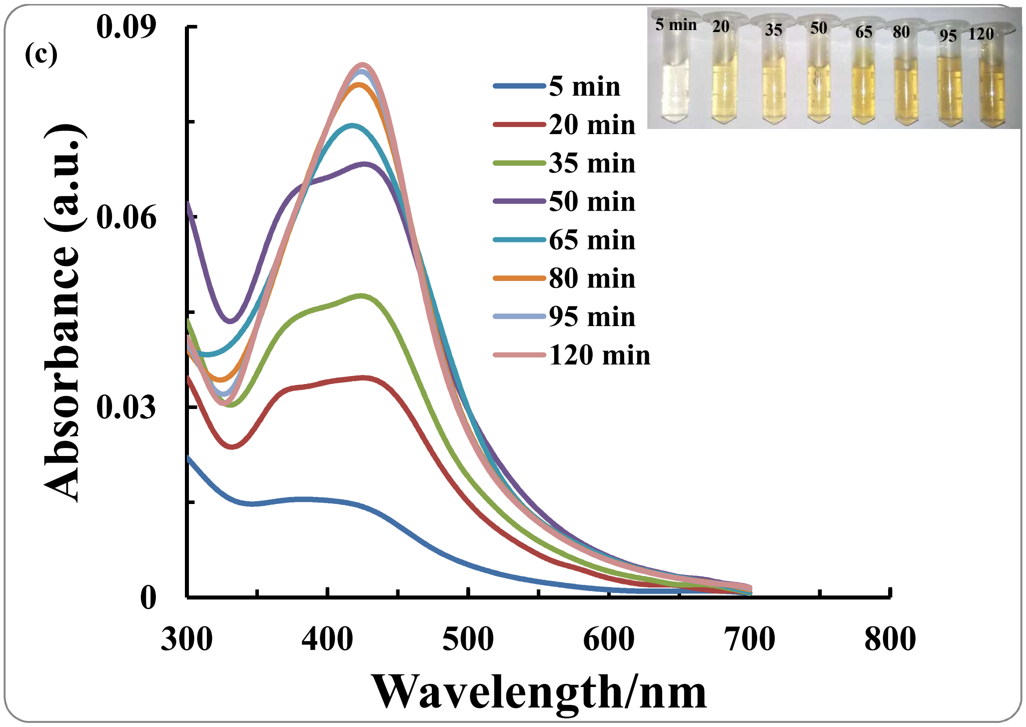

Figure 1. SPR spectra of C-SNSs showing the effect of (a) pH, (b) volume of clove seed extract, and (c) reaction time on the stability of C-SNSs. Inset images show the change in color by pH, volume and time, respectively.

Characterization of C-SNSs

UV-vis spectra of $AgNO_3$, clove seed extract, and C-SNSs solutions are shown in Figure 2. The $AgNO_3$ and clove seed extract did not give any peak in the region of 350-500 nm. A new SPR band appeared at 424 and 407 nm at pH 4.5 and 11.5 respectively, which confirms that the Ag^+ ions were reduced to C-SNSs in presence of clove seed extract. The size and morphology of C-SNSs were investigated by TEM image at pH 4.5 (Figure S1a) and SEM image at pH 11.5 (Figure 3a). The average diameter of C-SNSs observed was 38 nm at pH 4.5 and 24 nm at pH 11.5. Observations are in agreement with the SPR and zeta sizer results (Figure 2 and Figure S2). It is apparent from TEM and SEM images that particles are spherical and well dispersed in aqueous phase. Surface charge of C-SNSs was measured by zeta potential analyzer. Zeta potential of C-SNSs was –35 mV at pH 4.5 which increased to –46.3 mV at pH 11.5 (Figure S3a&c). This increased charge accumulated upon the surface of C-SNSs and is responsible for electrostatic stability of C-SNSs[47]. On the basis of the present study and earlier reports, we propose a probable mechanism for the synthesis of C-SNSs which is shown in Scheme 1. Eugenol is the main constituent of clove seed extract[48]. In eugenol, at ortho and para position of –OH, two electron withdrawing groups methoxy and allyl are present. Due to the effect of these two groups eugenol is able to release a hydroxyl proton and get converted into its anionic form. The anionic form of eugenol is further stabilized by two resonating structures. So, due to inductive effect of two electron withdrawing groups and tendency to form two stable resonating structures, eugenol is able to release two electrons simultaneously, one electron from the β-carbon of the resonating structure and the other from the CH_2 group next to the double bond due to increase in charge density. These two electrons are responsible for the reduction of $2Ag^+$ ions into 2Ag atoms. These neighboring Ag atoms collide with each other to form C-SNSs.

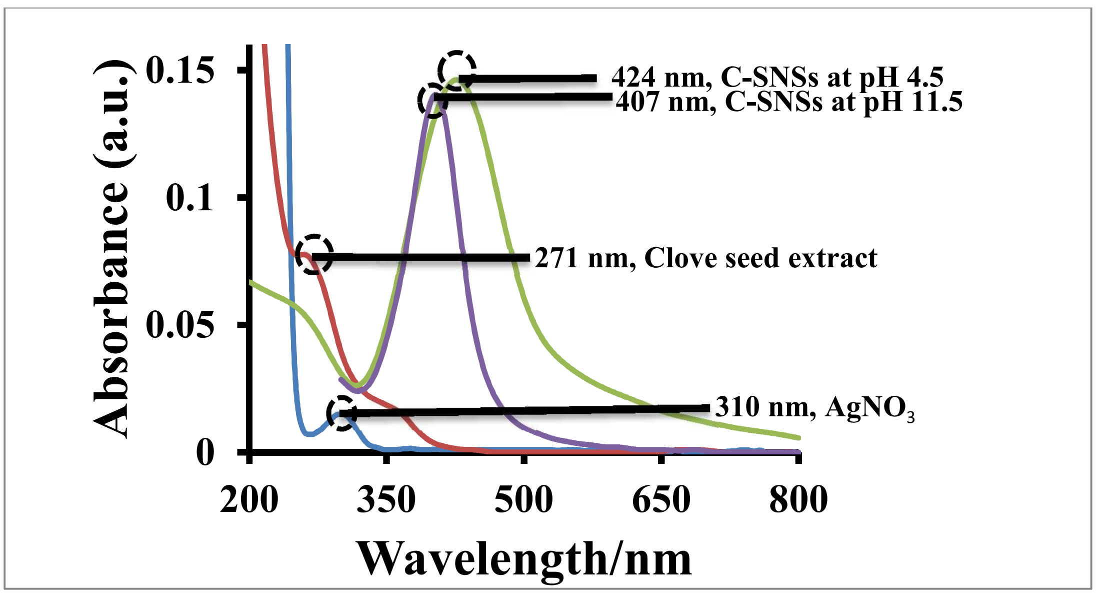

Figure 2. SPR spectra of $AgNO_3$ solution, clove seed extract, C-SNSs at pH 4.5 and C-SNSs at pH 11.5.

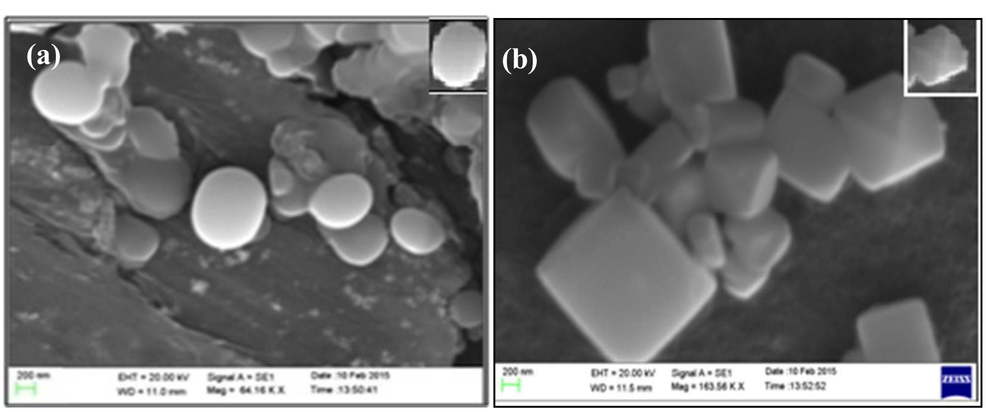

Figure 3. SEM images of C-SNSs at pH 11.5 in the absence(a); inset shows the spherical shape of spheres, and presence (b) of Mn(II) ions; inset shows square pyramidal particles.

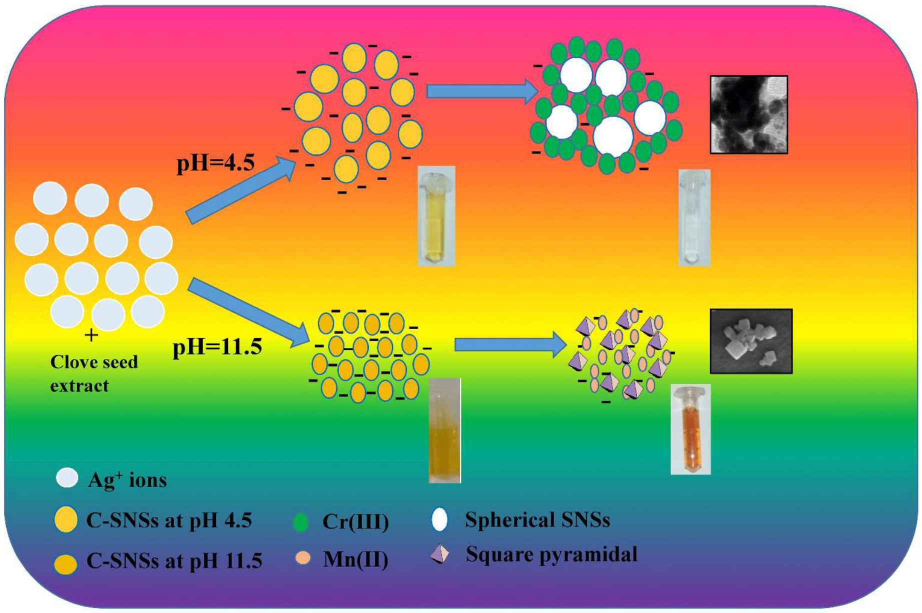

Scheme 1. Schematic illustration of the formation process of C-SNSs and its interaction with Cr(III) and Mn(II).

Selectivity of the detection method

The selectivity of detection probe was evaluated for Cr(III) and Mn(II) in the presence of other environmentally relevant metal ions including Ca(II), Cd(II), Cu(II), Hg(II), Zn(II), Ni(II), Pb(II), K(I), Co(II), Fe(III), Cr(VI), Ba(II), Mn(II), Al(III) and Cr(III). Each experiment to determine selectivity was conducted in triplicate.

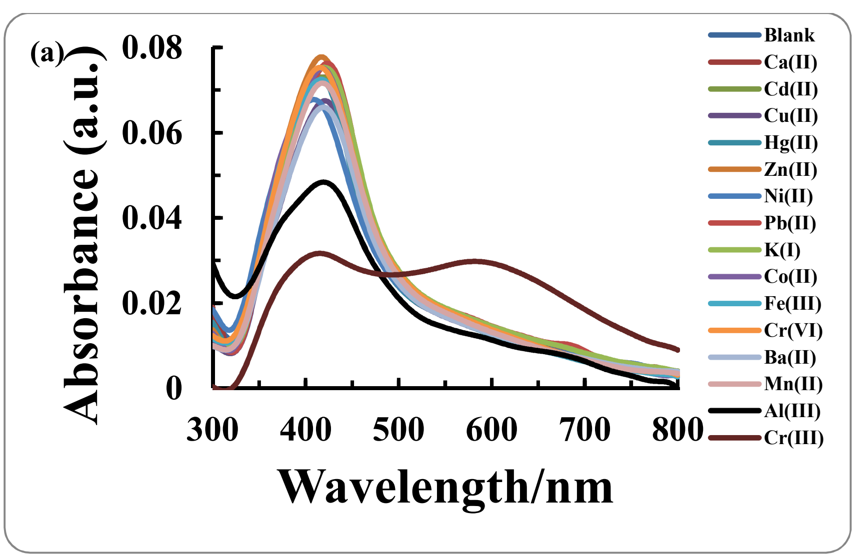

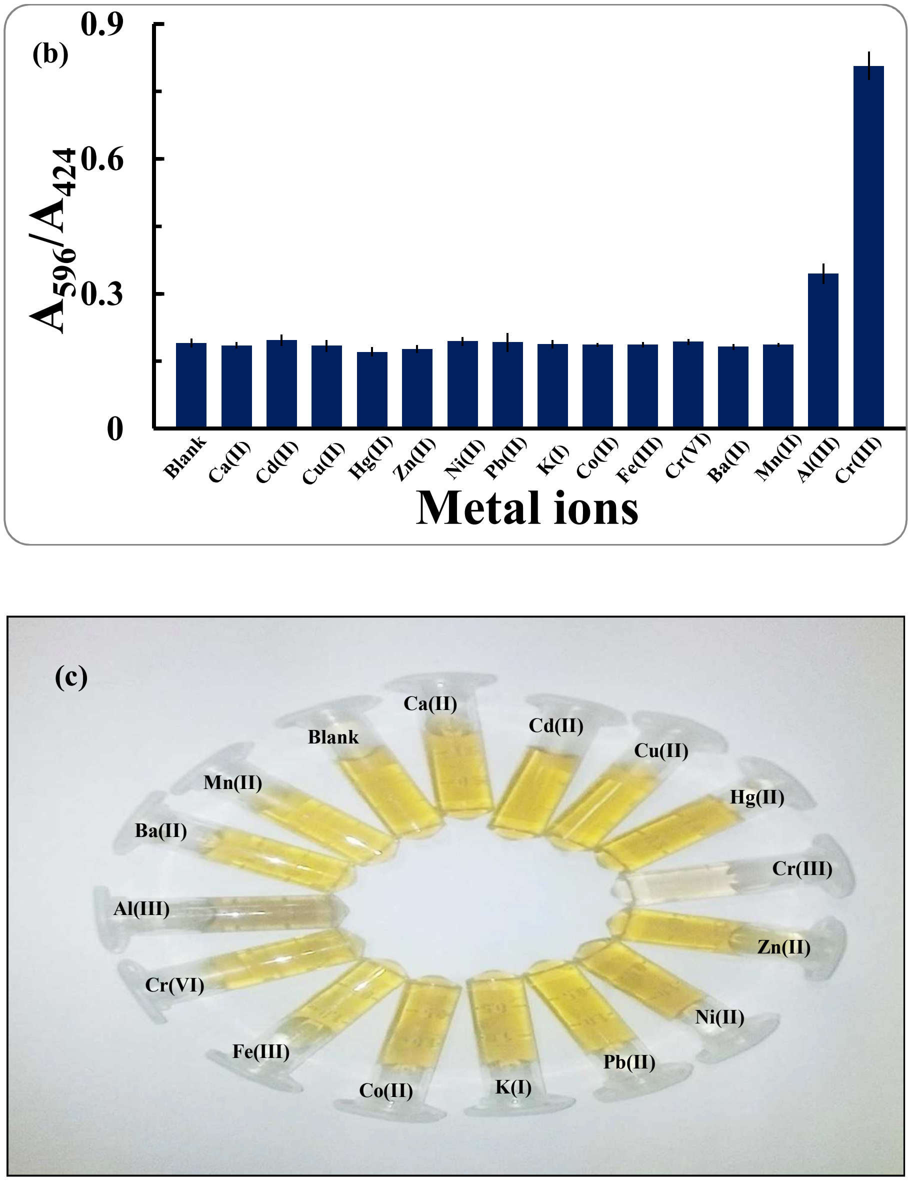

Figure 4. Selectivity of synthesized C-SNSs probe at pH 4.5 for the Cr(III); (a) SPR spectra of different metal ions, (b) bar diagram show the specificity of C-SNSs based probe for the Cr(III), error bars represent standard deviation from three repeated experiments, and (c) optical images of C-SNSs in the presence of different metal ions.

As shown in Figure 4a, at pH 4.5, there is the generation of a new peak at 596 nm upon addition of Cr(III); the presence of other metal ions did not show any significant change in SPR spectra. The selectivity of probe towards Cr(III) at pH 4.5 was further quantified by plotting absorption intensity ratio ($A_{596/424}$) of C-SNSs against concentration of metal ions (Figure 4b). The Cr(III) induced value of $A_{596/424}$ was much larger than observed for other metal ions, which can be used to show distinctive interaction of Cr(III) with C-SNSs.

However, the absorbance ratio for Al(III) ion is higher than other metal ions but significantly smaller than Cr(III) ion. This indicates that the C-SNSs probe is less selective for Al(III) than Cr(III) ion. The generation of a new peak and augmentation of value of $A_{596/424}$ is due to interaction between Cr(III) and C-SNSs which was further confirmed by change in color from light yellow to colorless observed by the naked eye as shown in Figure 4c. The possible mechanism for the detection of Cr(III) ions based on clove seed extract shown in Scheme 1. Clove seed extract composes phenolic compounds such as, eugenol, gallic acid, flavanoids, hydroxyl cinnamic acids and hydrolysable tannins[49]. Phenolic hydroxyl compounds have high affinity for Cr(III) ion[42]. According to the outer electron configuration of $3d^3 4s^0 4p^0$, Cr(III) ion has a smaller size, higher effective nuclear charge and stronger chelating tendency than other metal ions. Hence, it acts as a hard Lewis acid and can easily co-ordinate with the negatively charged oxygen of poly phenols. Co-ordination causes decrease in zeta potential of C-SNSs from -35 mV to -2.0 mV (Figure S3b). This large decrease in potential shows strong binding of Cr(III) with C-SNSs which results in almost complete neutralization of C-SNSs surface and hence induces aggregation of C-SNSs.

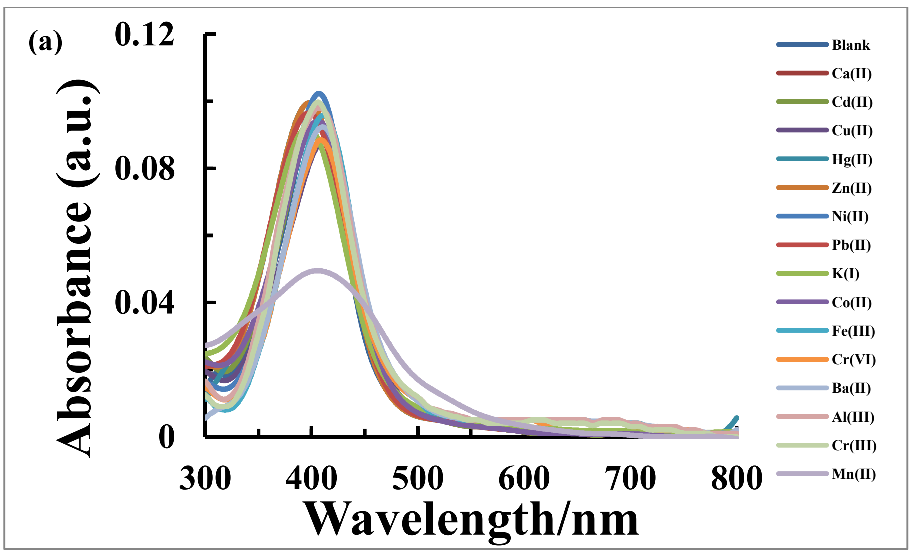

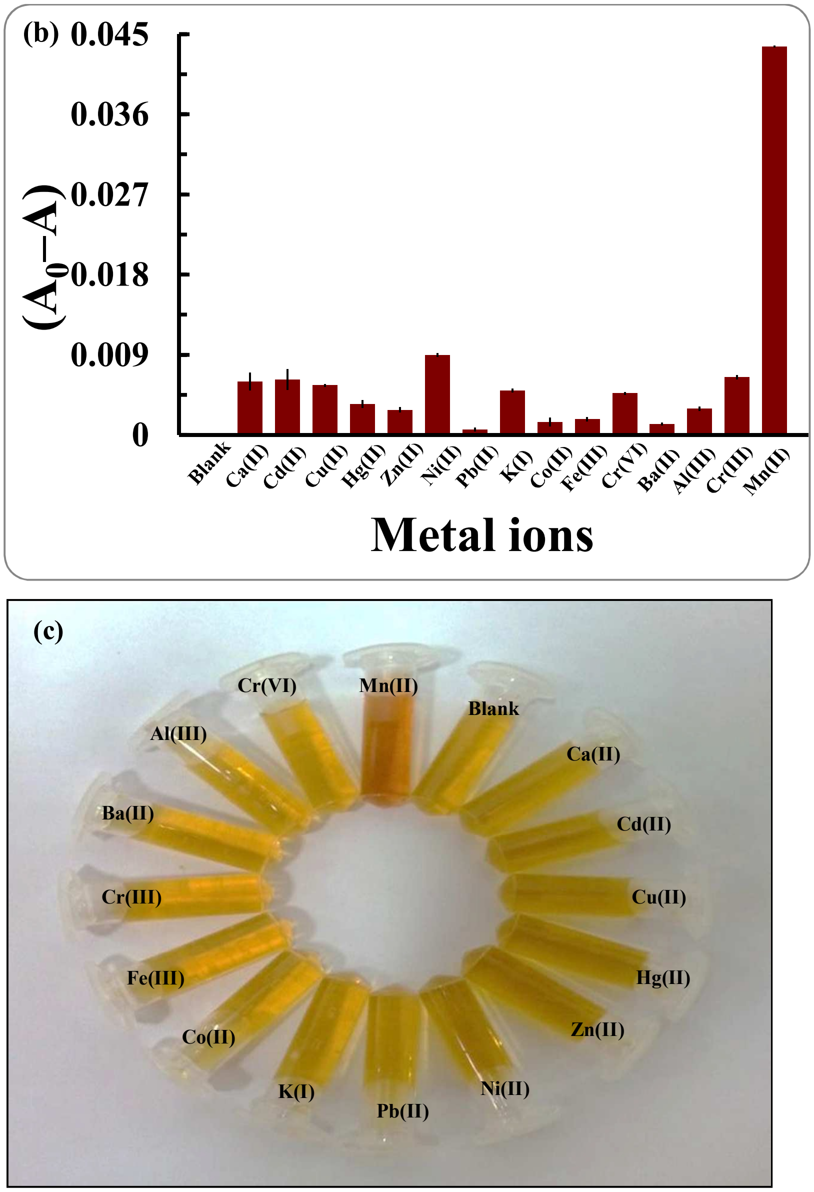

Figure 5. Selectivity of synthesized C-SNSs probe at pH 11.5 for the Mn(II) ions; (a) SPR spectra, (b) bar diagram shows the specificity of C-SNSs based probe for Mn(II) in comparison to other metal ions, error bars represents standard deviation from three repeated experiments and (c) optical images of C-SNSs in presence of different metal ions.

Similarly, the detection probe at pH 11.5 shows a distinctive change in the SPR spectra upon addition of Mn(II) ion, whereas no change was observed in the presence of other metal ions (Figure 5a). The selectivity is further explained by Figure 5b which is a plot of different metal ions vs A_0-A (A_0 = is the absorbance of C-SNSs in the absence of metal ions, A = is the absorbance of C-SNSs in presence of metal ions). The value of A_0-A for Mn(II) is much higher than other metal ions which also suggests better selectivity of C-SNSs probe for Mn(II) ions. It can be seen from Figure 5c that only Mn(II) induced aggregation of C-SNSs causes color change from dark yellow to reddish brown while co-existing metal ions do not show color change. The selectivity of C-SNSs for Mn(II) at pH 11.5 is explained on the basis of electrostatic interaction of Mn(II) with C-SNSs which is responsible for decreasing interparticle distance to induce aggregation (Scheme 1). Mie theory also states that as the distance between the particles become smaller than the sum of their radii, SPR band exhibits low intensity and broadening[50,51]. Electrostatic interaction between C-SNSs and Mn(II) ions is shown by decrease in zeta potential value from -46.6 mV to -15 mV (Figure S3d). The interaction of Mn(II) changes C-SNSs from spherical to square pyramidal. This morphology transition indicates that the spherical morphology which was composed completely of ionic interactions, was disturbed by the addition of Mn(II)[52].

Sensitivity of Probe

To evaluate the lower LODs of the synthesized probe, different concentrations of Cr(III) and Mn(II) ions were added into the C-SNSs probe solutions.

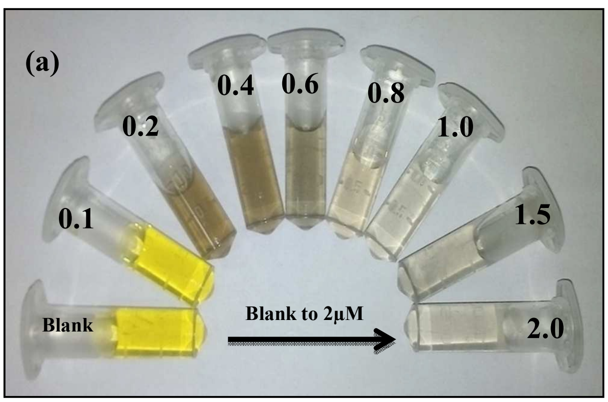

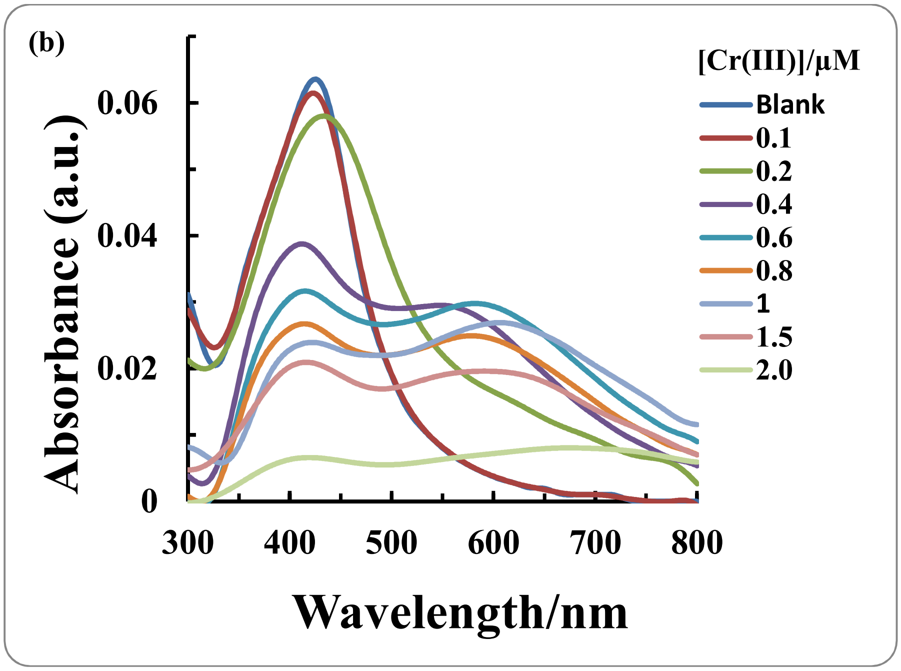

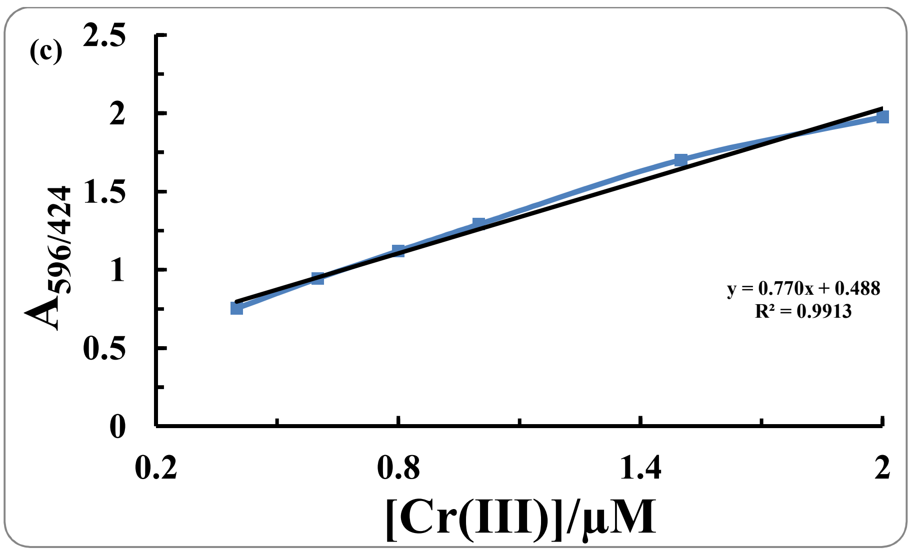

Figure 6. (a) Optical images and (b) SPR spectra of C-SNSs based detection system in the presence of various concentrations of Cr(III) ranging from 0.1−2.0 μM at pH 4.5, (c) Plot of $A_{596/424}$ as the function of concentration of Cr(III) which shows linearity of $A_{596/424}$ values of C-SNSs probe solution at 424 nm.

The colorimetric results show that on increasing the concentration of Cr(III) from 0.2−2.0μM, a continuous change in color from light yellow to colorless was observed as shown in Figure 6a. The LOD for Cr(III) ion is 0.2 μM. However, the reaction rates are different but the final results are almost same at different concentrations of Cr(III) ions because the reaction of Cr(III) ions with C-SNSs proceeds until the C-SNSs aggregate completely.

SPR spectra of the detection system on interaction with various concentrations of Cr(III) ions at pH 4.5 are shown in Figure 6b. The addition of Cr(III) to the detection system not only causes an intensity decrease and red shifting of characteristic SPR band but also the generation of a new sister peak at 596 nm. Finally, this peak disappears at the final concentration of 2.0 μM. As shown in Figure 4c the Al(III) also showed a change in color of C-SNSs. We plotted the ratio of $A_{596/424}$ against the concentration of Al(III) and Cr(III) metal ions, respectively to quantitatively describe the responsive sensitivity of C-SNSs toward Al(III) and Cr(III) at pH 4.5. From the ratiometric plot (Figure S4) it is apparent that the Cr(III) ion above concentration 0.2 μM induces interparticle association of C-SNSs which leads to a change in their SPR spectra. However, Al(III) showed a slight change at concentration higher than 0.6 μM. Therefore, the C-SNSs show much higher sensitivity for Cr(III) than Al(III). These observations could be used for the quantitative measurement of the Cr(III) in the solution (Figure 6c). The concentration of Cr(III) ions in the range of 0.4–2.0 μM were employed to construct the calibration curve which showed a linear correlation (R^2=0.9913) up to 2.0 μM.

Similarly, a change in color from dark yellow to reddish-brown was observed as the concentration of Mn(II) increased from 0.2-2.0 μM as shown in Figure7a. The LOD of the detection system for Mn(II) is 0.2 μM. SPR spectra of the detection system on interaction with various concentrations of Mn(II) ions at pH 11.5 are shown in Figure 7b. With increasing concentration of Mn(II), there was a gradual shift observed in the SPR band of C-SNSs toward a longer wavelength with line broadening and decrease of intensity. Finally, the peak disappears at the concentration of 2.5 μM. Figure 7c reveals there is a linear relationship between absorption intensity changes and the concentration of Mn(II) over a range of 0.2−2.5 μM with a linear correlation value (R^2) of 0.9909.

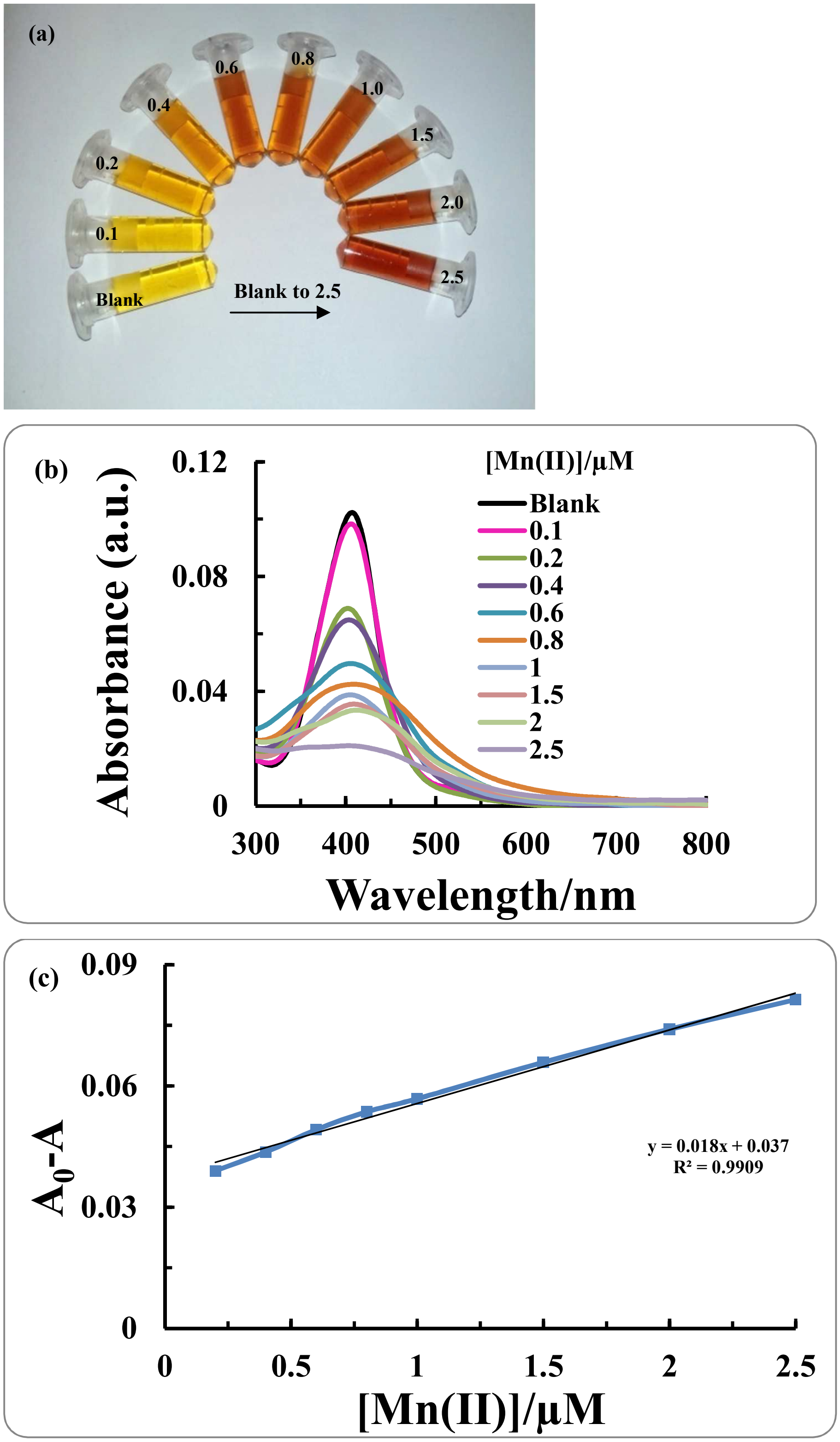

Figure 7. (a) Optical images, (b) SPR spectra of C-SNSs based detection system in the

presence of various concentrations of Mn(II) ranging from 0.1 to 2.5 at pH 11.5, (c) plot of A_0-A versus concentration of Mn(II) at pH 11.5.

Table 1 Comparison of the performance of various sensors for Cr(III) and Mn(II)

Detection system	**Metal ion**	**LOD/µM (naked eye)**	**Ref.**
PMMA@Au NPs	Cr(III)	40	53
Citrate-AuNPs	Cr(III), Cr(VI)	4.0	13
NTP@AuNPs	Cr(III)	1.4	54
XT-AuNPs	Cr(III)	3.0	42
Dopa-AuNPs	Mn(II)	5.0	10
$Na_4P_2O_7$ and HPMC SNSs	Mn(II)	0.50	33
C-SNSs	Cr(III), Mn(II)	0.20	Present work

The performance of biocompatible C-SNSs based detection system for Cr(III)and Mn(II) ions also compares with reported sensors (Table 1). The sensitivity and ease of synthesis of our proposed detection system makes it more advantageous over other systems.

Detection of Cr(III) and Mn(II) ions in tap water samples

To promote the effectiveness of our detection system, the probe prepared at pH 4.5 and 11.5 was tested on a tap water sample collected from household source. Contamination by Cr(III) and Mn(II) in tap water sample was lower than LOD of synthesized probe, thus the tap water sample was contaminated with standard solutions of Cr(III) and Mn(II). Figure 8a&b show the colorimetric response of the detection probe in tap water with Cr(III) and Mn(II). On increasing the concentration of corresponding metal ion, the probe response linearly increased. The response of the detection probe was quite similar for both mill-Q water and tap water which suggests that the Cr(III) and Mn(II) can be detected in tap water without interfering contaminants. At low concentration the detection system shows a good linearity with R^2 values of 0.9926 and 0.9942 for Cr(III) and Mn(II), respectively (Figure S5a&b). To further demonstrate the applicability of C-SNSs probe the recovery experiment was performed with Cr(III)and Mn(II) contaminated tap water (1.5 and 2.0 μM). The average percentage recovery of the C-SNSs probe was observed in the range of 91.32 to 114.50 (Table 2). This confirms the utility of synthesized C-SNSs probe for the detection of Cr(III) and Mn(II) ions in real water samples.

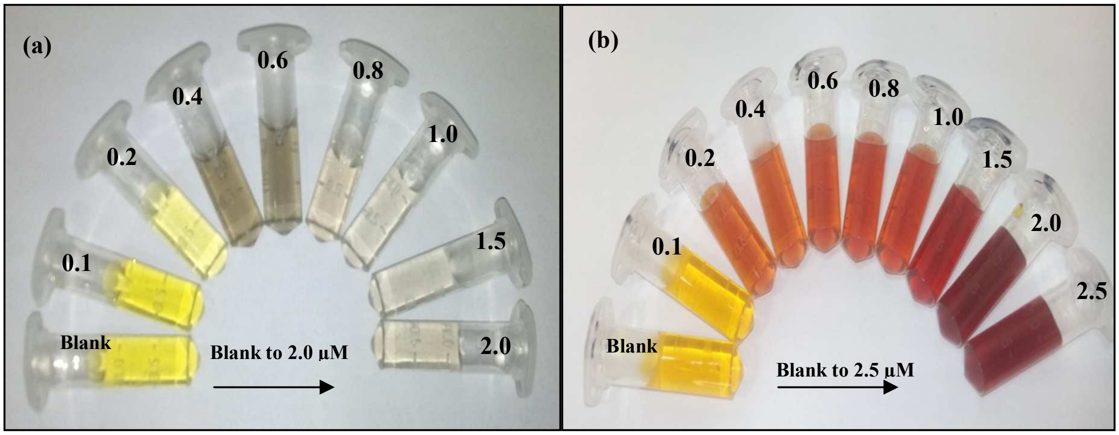

Figure 8. Colorimetric response of Cr(III) ion (a) and Mn(II) ion (b) in tap water samples.

Table 2 Detection of Cr(III) and Mn(II) in tap water sample by our prepared C-SNSs probe

Sample	**[M^{n+}]/µM**	**Cr(III) and Mn(II) found (mean±E, n=3)**	**Recovery (%)**
Tap water	Blank	0	-
Cr(III)	1.5	1.47 ± 0.10	98±6.6
	2.0	1.92±0.05	96±2.5
Tap water	Blank	0	-
Mn(II)	1.5	1.39±0.02	92.66±1.34
	2.0	2.2±0.09	110±4.5

3. CONCLUSIONS

We have established the use of clove seed extract as a reducing as well as stabilizing agent for the synthesis of SNSs. The prepared C-SNSs are highly stable in aqueous medium and do not show any signs of aggregation up to a month. The prepared SNSs were characterized by UV-vis, TEM, SEM and zeta potential techniques. The shape and size of SNSs was optimized by varying pH, reaction time and concentration of clove seed extract. The C-SNSs based detection system has high sensitivity (0.2 μM) for both Cr(III) and Mn(II) ions over other alkali, alkaline earth and transition metal ions. The metal ion induced aggregation of C-SNSs causes the change in color from light yellow to colorless for Cr(III) and dark brown to reddish brown for Mn(II). The synthesized probe does not require any surface modifications by DNA, thiol containing groups, any fluorescent compounds or dyes, nor does it require optimizing temperature conditions for detection. The ease of preparation, biocompatibility and ability to simultaneously determine two metal ions make it useful and easy to apply. This work will provide a simple and plausible route in the application of nanoprobe for the detection of heavy metal ions in tap water samples.

ACKNOWLEDGEMENTS

We gratefully acknowledge support from the Ministry of Human Resource Development Department of Higher Education, Government of India under the scheme of Establishment of Centre of Excellence for Training and Research in Frontier Areas of Science and Technology (FAST), for providing the necessary financial support to carry out this study vide letter No, F. No. 5-5/201 4-TS.Vll. The authors would like to thank University of Rajasthan, Jaipur providing SEM facility.

References

1. L. S. Walekar, A. H. Gore, P. V. Anbhule, V. Sudarsan, S. R. Patil and G.B. Kolekar, *Anal. Methods,* 2013, **5**, 5501-5507.
2. M. Sa'idi, *Int. J. Environ. Sci.,* 2010, **1**, 666-676.
3. L. Beqa, A. K. Singh, S.A. Khan, D. Senapati, S. R. Arumugam and P.C. Ray, *Appl. Mater. Interfaces,* 2011, **3**, 668–673.
4. G. Aragay, G. Alarcon, J. Pons, M. Font-Bardía and A. Merkoci, *J. Phys. Chem. C,* 2012, **116**, 1987–1994.
5. J. Zhang, L. Zhang, Y. Wei, J. Chao, S. Wang, S. Shuang, Z. Cai and C. Dong, *Anal. Methods,* 2013, **5**, 5549–5554.
6. M. Elavarasi, A. Rajeshwari, N. Chandrasekaran and A. Mukherjee, *Anal. Methods,* 2013, **5**, 6211–6218.
7. A. Fargasova, *Ecol. Chem. Eng. S,* 2008, **15**, 335-348.
8. K. Farhadi, M. Forough, R. Molaei, S. Hajizadeh and A. Rafipour, *Sensor. Actuat. B-Chem.,* 2012, **161**, 880–885.
9. D. C. Dorman, M. F. Struve, R. A. James, B. E. McMnus, M. W. Marshall and B. A. Wong, *Toxicol. Sci.,* 2001, **60**, 242–251.
10. K. B. Narayanan and H. H. Park, *Spectrochim. Acta. A,* 2014, **131**, 132–137.
11. A. B. Bowman, G. F. Kwakye, E. H. Hernández and M. Aschner, *J. Trace. Elem. Med. Biol.*, 2011, **25**, 191-203.
12. USEPA, Manganese, United States Environmental Protection Agency, Integrated Risk Information System (IRIS), Washington, DC, 1997.
13. Y. Liu and X. Wang, *Anal. Methods,* 2013, **5**, 1442–1448.

14. Y. Zhou, H. Zhao, C. Li, P. He, W. Peng, L. Yuan, L. Zeng and Y. He, *Talanta,* 2012, **97**, 331–335.

15. J. P. Mettres, R. O. Kadara and C. E. Banks, *Analyst,* 2012, **137**, 896-902.

16. S. A. Miscoria, C. Jacq, T. Maeder and R. M. Negri, *Sensor. Actuat. B-Chem*., 2014, **195**, 294-302.

17. I. Michaud-Soret, A. Adrait, M. Jaquinod, E. Forest, D. Touati and J. M. Latour, *FEBS Letters,* 1997*,* **413**, 473-476.

18. E. Weldy, C. Wolff, Z. Miao and H. Chen, *Sci. Justice,* 2013, **53**, 293-300.

19. S. Sadeghi and A. Z. Moghaddum, *Anal. Methods,* 2014*,* **6**, 4867-4877.

20. H. L. Sun, H. M. Liu and S. J. Tsai, *J. Chromatogr. A.*, 1999, **857**, 351–357.

21. R. Kachadourian, R. Menzeleev, B. Agha, S. B. Bocckino and B. J. Day, *J. Chromatogr. B Analyt. Technol. Biomed. Life Sci.*, 2002, **767**, 61–67.

22. A. Calleja, V. Ríos, M. Luque, R. Ostos, A. Grilo, A. M. Cameán and L. Moreno, *J. Toxins,* 2014, **1**, 1-10.

23. R. E. Wolf, J. M. Morrison and M. B. Goldhaber, *J. Anal. At. Spectrom.,* 2007, **22**, 1051–1060.

24. Y. Inoue, T. Sakai and H. Kumagai, *J. Chromatogr. A,* 1997, **706**, 127-136.

25. M. Golasik, M. Herman, W. Piekoszewski, E. Gomółka, G. Wodowski and S. Walas, *Anal. Lett.,* 2014, **47**, 1921–1930.

26. S. K. Soni, P. R. Selvakannan, S. K. Bhargava and V. Bansal, *Langmuir*, 2012, **28**, 10389-10397.

27. M. Sperling, S. Xu and B. Welz, *Anal. Chem.,* 1992, **64**, 3101–3108.

28. Y.-X. Gao, J.-W. Xin, Z.-Y. Shen, W. Pan, X. Li and A.-G. Wu, *Sensor. Actuat. B Chem.,* 2013, **181**, 288-293.

29. M. Elavarasi, M. L. Paul, A. Rajeshwari, N. Chandrasekaran, A. B. Mandal and A. Mukherjee, *Anal. Methods,* **2012**, 4, 3407-3412.

30. H. Zhang, Q. Liu, T. Wang, Z. Yun, G. Li, J. Liu and G. Jiang, *Anal. Chim. Acta,* 2013, **770**, 140–146.

31. Q. Q. Fu, Y. Tang, C. Y. Shi, X. L. Zhang, J. J. Xiang and X. Liu, *Biosens. Bioelectron.,* 2013, **49**, 399–402.

32. R. Hu, L. Zhang and H. Li, *New J. Chem.,* 2014, **38**, 2237–2240.

33. G. Wu, C. Dong, Y. Li, Z. Wang, Y. Gao, Z. Shen and A. Wu, *RSC Adv.,* 2015, **5**, 20595– 20602.

34. J. Xin, L. Miao, S. Chen and A. Wu, *Anal. Methods,* 2012, **4**, 1259-1264.

35. L. Zhao, Y. Jin, Z. Yan, Y. Liu and H. Zhu, *Anal. Chim. Acta.,* 2012, **731**, 75-81.

36. S. I. Hughes, S. S. R. Dasary, A. K. Singh, Z. Glenn, H. Jamison, P. C. Ray and H. Yu, *Sensor. Actuat. B-Chem.,* 2013, **178**, 514–519.

37. Y. Zhou, Y.-S. Li, X. L. Tian, Y. Y. Zhang, L. Yang, J. H. Zhang, S. Y. Wang, X. R. Lu, H. L. Ren and Z. S. Liu, *Sensor. Actuat. B-Chem.,* 2012, **161**, 1108–1113.

38. H. R. Ghorbani, A. A. Safekordi, H. Attar and S. M. R. Sorkhabadi, *Chem. Biochem. Eng. Q.,* 2011, **25**, 317–326.

39. S. S. Ravi, L. R. Christena, N. S. Subramanian and S. P. Anthony, *Analyst,* 2013, **138**, 4370-4377.

40. C. K. Balavigneswaran, T. S. J. Kumar, R. M. Packiaraj and S. Prakash, *Appl. Nano. Sci.,* 2014, **4**, 367–378.

41. M. Gondwal and G. J. N. Panta, *Int. J. Pharm. Bio. Sci.,* 2013, **4**, 635–643.

42. W. Ha, J. Yu, R. Wang, J. Chen and Y.-P. Shi, *Anal. Methods*, 2014, **6**, 5720-5726.

43. A. K. Singh, M. Talat, D. P. Singh and O. N. Srivastava, *J. Nanopart. Res.,* 2010, **12**, 1667–1675.

44. U.S. EPA, Integrated Risk Information System (IRIS) on Chromium III. National Center for Environmental Assessment, Office of Research and Development: Washington, DC, 1999.

45. U.S. EPA, Drinking Water Health Advisory for Manganese. U.S. Environmental Protection Agency Office of Water, Health and Ecological Criteria Division Washington, DC, 2004.

46. H. Kaur, S. Kaur and M. Singh, *Biologia,* 2013, **68**, 1048-1053.

47. C. C. Huang and H. T. Chang, *Chem. Commu.,* 2007, (12), 1215-1217.

48. L. Jirovetz, G. Buchbauer, I. Stoilova, A. Stoyanova, A. Krastanov and E. Schmidt, *J. Agric. Food. Chem.,* 2006, **54**, 6303–6307.

49. D. F. Cortés-Rojas, C. R. F. S. Souza and W. P. Oliveira, *Asian Pac. J. Trop. Biomed.,* 2014, **4**, 90-96.

50. M.-C. Daniel and D. Astruc, *Chem. Rev.,* 2004, **104**, 293–346.

51. S. K. Ghosh and T. Pal, *Chem. Rev.,* 2007, **107**, 4797–4862.

52. N. Vilvamani, S. Deka and T. Gupta, *Adv. Mat. Lett.,* 2013, **4**, 252-260.

53. J. Li, C. Han, W. Wu, S. Zhang, J. Guo and H. Zhou, *New J. Chem.* 2014, **38**, 717-722.

54. Y.-C. Chen, I-L. Lee, Y.-M. Sung and S.-P. Wu, *Sensor. Actuat. B-Chem.,* 2013, **188**, 354-359.